# Synthesis, Crystal Structure, and Thermal Decomposition Kinetics of the Complex of Dysprosium Benzoate with 2,2′-Bipyridine

**Liang Tian,[†,‡] Ning Ren,[§] Jian-Jun Zhang,*[,†] Shu-Jing Sun,[†,‡] Hong-Mei Ye,[†,‡] Ji-Hai Bai,[||] and Rui-Fen Wang[‡]**

Experimental Center, Hebei Normal University, Shijiazhuang 050016, P. R. China, College of Chemistry & Material Science, Hebei Normal University, Shijiazhuang 050016, P. R. China, Department of Chemistry, Handan College, Handan 056005, P. R. China, and Department of Compute, Hebei Normal College of Science and Technology, Qinhuangdao, 066600 P. R. China

The complex $[Dy(BA)_3bipy]_2$ (BA = benzoate; bipy = 2,2′-bipyridine) was obtained and characterized by elemental analysis, molar conductance, infrared spectra (IR), ultraviolet spectra (UV), single-crystal X-ray diffraction, thermogravimetry, and differential thermogravimetry (TG-DTG) techniques. The crystal is monoclinic with space group $P2(1)/n$. The unit cell parameters are: $a = 14.1114(8)$ Å, $b = 15.3743(9)$ Å, $c = 25.8887(14)$ Å, $\alpha = 90°$, $\beta = 103.4410(10)°$, $\gamma = 90°$. Two $Dy^{3+}$ ions are connected by four carboxylic groups through a bridging bidentate mode. The thermal decomposition behavior of the title complex under a static air atmosphere was studied using the TG-DTG, scanning electron microscopy (SEM), and IR techniques. The nonisothermal kinetics was investigated by using the double equal-double steps method and the Starink method. The mechanism function of the first decomposition step was determined. The thermodynamic parameters ($\Delta H^{\neq}$, $\Delta G^{\neq}$, and $\Delta S^{\neq}$) and kinetic parameters (activation energy $E$ and the pre-exponential factor $A$) were also calculated.

## Introduction

In recent years, carboxylate complexes have drawn great attention among scholars due to their special structures and unique propetries.[1−8] Especially rare-earth metals and aromatic carboxylic acids may form network structures and net layer structures.[9] For these complexes, oxygen atoms can coordinate to metal ions via different modes, including monodentate, bidentate chelating, bidentate bridging, tridentate chelating−bridging, etc. In addition to the special structures of these complexes, much attention has been increasingly attracted by their thermal decomposition and nonisothermal kinetics. The study of the thermal behavior will provide valuable information for choosing new functional materials with better stability.

In previous studies,[10−22] a series of Sm, Eu, Tb, and Dy complexes with benzoic acid or benzoate derivatives and nitrogen-containing ligands were prepared, and their crystal structures, thermal decomposition behaviors, and nonisothermal kinetics were also reported. As an extension of these studies, the complex $[Dy(BA)_3bipy]_2$ was synthesized. The crystal structure and thermal decomposition mechanism were determined by the TG-DTG, SEM, and IR techniques. The nonisothermal kinetics was studied by using the double equal-double steps method[23] and the Starink method.[24]

## Experimental Section

***Chemicals and Apparatus.*** $Dy_2O_3$ (≥ 99.99 %), benzoic acid, and 2,2′-bipyridine were obtained from commercial sources and used without further purification.

The content of carbon, hydrogen, and nitrogen was acquired on a Vario-EL III element analyzer, while the metal content was assayed using an EDTA titration method. Infrared spectra were recorded at room temperature from (4000 to 400) $cm^{-1}$ using a Perkin-Elmer FTIR-1730 spectrometer with the KBr disk technique. The ultraviolet spectra were recorded on a Shimadzu 2501 spectrophotometer in DMSO (DMSO = dimethylsulfoxide). The molar conductance was determined with a Shanghai DDS-307 conductivity meter. The single crystal X-ray diffraction data were obtained by a Bruker Apex II CCD diffractometer with graphite-monochromated Mo Kα radiation ($\lambda = 0.71073$ Å) at 293 K using the $\varphi-\omega$ scan technique in the range of $1.66° \le \theta \le 26.00°$. A semiempirical absorption correction with SADABS was applied. The structure was solved by direct methods using the SHELXS-97 program and refined by full-matrix least-squares on $F^2$ using the SHELXL-97 program to $R_1 = 0.0646$ and $wR_2 = 0.1361$. The TG-DTG experiments of the title complex were achieved using a Perkin-Elmer TGA7 thermogravimetric analyzer. The heating rate was (3, 5, 7, 10, and 15) $K \cdot min^{-1}$ from ambient to 1223 K under a static air atmosphere. A small amount of the sample was uniformly dispersed in the sample holder, and a gold layer was sprayed for 15 min with Hitachi IB-5. Then, the sample was observed by a Hitachi S-570 scanning electron microscope.

***Preparation of the Title Complex.*** $DyCl_3 \cdot 6H_2O$(0.2 mmol), benzoic acid (0.6 mmol), and 2,2′-bipyridine (0.2 mmol) were dissolved in open beakers (50 mL), respectively, with 95 % $C_2H_5OH$ solution. The pH value of the benzoic acid solution was adjusted to 6 to 7 with NaOH ($1 mol \cdot L^{-1}$). The two ligands were mixed, and the mixture was added dropwise into the $DyCl_3 \cdot 6H_2O$ solution, stirred using an electromagnetic stirrer continuously at room temperature for about 10 h, and then deposited for 12 h. Subsequently, the precipitates were collected by filtration and then dried in a desiccator. The colorless single crystals were obtained by slow evaporation of the mother solution at room temperature after about four weeks.

* Corresponding author. Tel.: +86-031186269373. Fax: +86-031186268405. E-mail: jjzhang6@126.com.
[†] Experimental Center, Hebei Normal University.
[‡] College of Chemistry & Material Science, Hebei Normal University.
[§] Handan College.
[||] Hebei Normal College of Science and Technology.

10.1021/je8006106 CCC: $40.75 
Published on Web 12/04/2008

**Table 1. Data of Elementary Analysis and Molar Conductivity for the Title Complex**

| complex $[Dy(BA)_3bipy]_2$ | C % | H % | N % | Dy % | $\Lambda/S \cdot cm^2 \cdot mol^{-1}$ |
|---|---|---|---|---|---|
| experimental values | 53.97 | 3.23 | 3.97 | 23.27 | 12.20 |
| theoretical values | 54.59 | 3.40 | 4.11 | 23.83 | - |

**Table 2. IR Absorption for the Ligands and Complex ($cm^{-1}$)**

| compounds | $\nu_{CN}$ | $\delta_{CC}$ | $\delta_{CH}$ | $\nu_{CO}$ | $\nu_{as}$ ($COO^-$) | $\nu_s$ ($COO^-$) | $\nu$ (RE−O) |
|---|---|---|---|---|---|---|---|
| bipy | 1578 | 992 | 757 | - | - | - | - |
| HBA | - | - | - | 1688 | - | - | - |
| $[Dy(BA)_3bipy]_2$ | 1599 | 1013 | 774 | - | 1636 | 1407 | 427 |

## Results and Discussion

***Elemental Analysis and Molar Conductance.*** The contents of C, H, N, and Dy of the title complex are listed in Table 1. It can be seen that the experimental results are in good accord with the theoretical data, which is identified as matching the empirical formula of $[Dy(BA)_3bipy]_2$. The molar conductance of the compound is also listed in Table 1, which indicates that the complex acts as a nonelectrolyte.

The title complex is colorless and can exist stably at room temperature in air. It is insoluble in water, ethanol, and acetone solution but freely soluble in DMSO and DMF (DMF = *N*,*N*-dimethylformamide) solution.

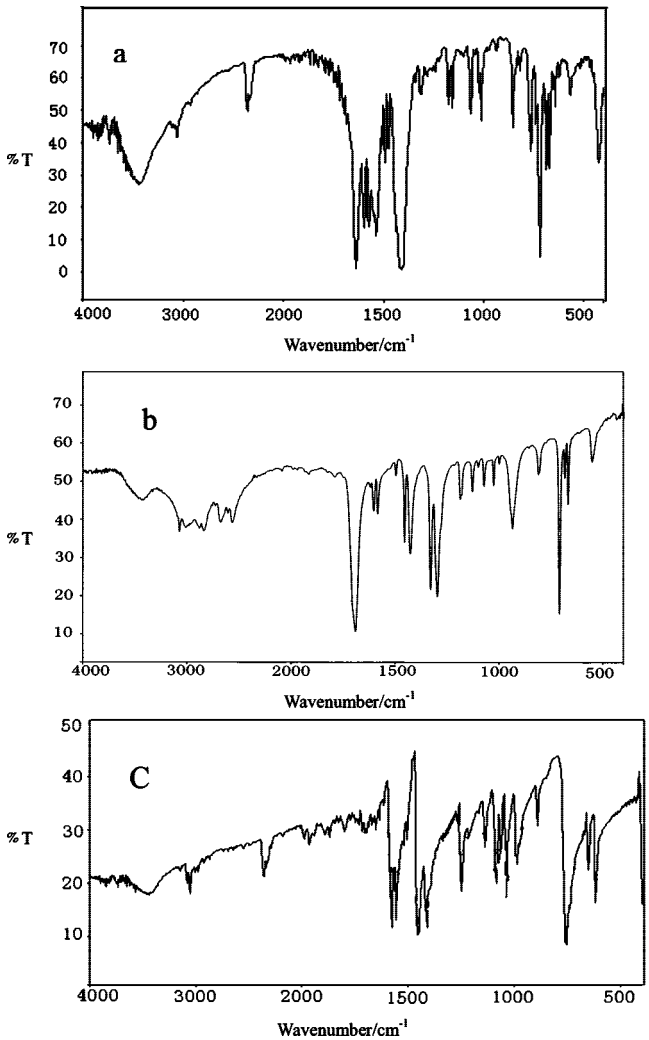


**Figure 1.** IR spectra of the title complex and the ligands: a, $[Dy(BA)_3bipy]_2$; b, HBA; c, bipy.

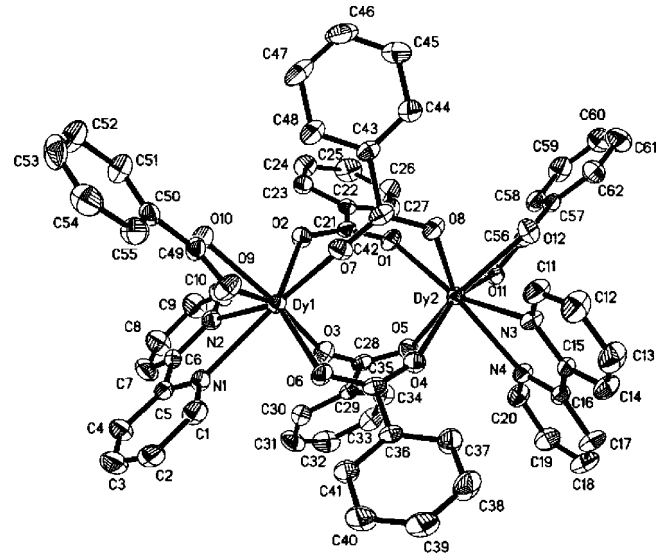


**Figure 2.** Moleculor structure of the title complex.

**Table 3. Crystal Data and Structure Refinement for the Title Complex**

| item | data |
|---|---|
| empirical formula | $C_{62}\ H_{46}\ Dy_2\ N_4\ O_{12}$ |
| formula weight | 1364.03 |
| temperature | 293(2) K |
| wavelength | 0.71073 Å |
| crystal system, space group | Monoclinic, *P*2(1)/*n* |
| unit cell dimensions | $a = 14.1114(8)$ Å, $\alpha = 90°$<br>$b = 15.3743(9)$ Å, $\beta = 103.4410(10)°$<br>$c = 25.8887(14)$ Å, $\beta = 90°$ |
| volume | 5462.8(5) $Å^{-3}$ |
| *Z*, calculated density | 4, 1.659 $Mg \cdot m^{-3}$ |
| absorption coefficient | 2.783 $mm^{-1}$ |
| *F*(000) | 2696 |
| crystal size | 0.467 × 0.410 × 0.083 mm |
| $\theta$ range for data collection | (1.62 to 26.00) ° |
| Limiting indices | $-11 \leqslant h \leqslant 17$, $-18 \leqslant k \leqslant 16$, $-31 \leqslant l \leqslant 31$ |
| Reflections collected/unique | 29589/10698 [*R*(int) = 0.1377] |
| completeness to $\theta = 26.00$ | 99.6 % |
| absorption correction | empirical |
| max. and min. transmission | 1.00000 and 0.47994 |
| refinement method | full-matrix least-squares on $F^{-2}$ |
| data/restraints/parameters | 10698/0/722 |
| goodness-of-fit on $F^2$ | 0.960 |
| final *R* indices [$I > 2o(I)$] | $R_1 = 0.0534$, $wR_2 = 0.1303$ |
| *R* indices (all data) | $R_1 = 0.0646$, $wR_2 = 0.1361$ |

***Infrared Spectra.*** The characteristic bands of the ligands and complex are displayed in Table 2. The IR spectra of the ligands and complex are shown in Figure 1. The characteristic absorp-

**Table 4. Selected Bond Lengths [Å] and Angles [°] for the Title Complex**

| | | | |
|---|---|---|---|
| Dy(1)−O(7) | 2.276(5) | Dy(1)−O(9) | 2.458(4) |
| Dy(1)−O(2) | 2.340(4) | Dy(1)−O(10) | 2.362(4) |
| Dy(1)−N(1) | 2.560(5) | Dy(1)−O(3) | 2.275(5) |
| Dy(1)−N(2) | 2.605(5) | Dy(1)−O(6) | 2.311(4) |
| O(7)−Dy(1)−O(10) | 91.58(17) | O(9)−C(49) | 1.264(8) |
| O(3)−Dy(1)−O(10) | 147.60(16) | O(10)−C(49) | 1.267(8) |
| O(6)−Dy(1)−O(10) | 133.89(16) | O(7)−Dy(1)−O(9) | 75.14(17) |
| O(2)−Dy(1)−O(10) | 81.80(15) | O(3)−Dy(1)−O(9) | 154.51(17) |
| O(7)−Dy(1)−O(2) | 77.85(16) | O(6)−Dy(1)−O(9) | 79.96(16) |
| O(7)−Dy(1)−N(2) | 153.19(16) | O(2)−Dy(1)−O(9) | 126.52(16) |
| O(3)−Dy(1)−N(2) | 73.50(17) | O(10)−Dy(1)−O(9) | 54.13(15) |
| O(6)−Dy(1)−N(2) | 125.98(17) | O(7)−Dy(1)−O(3) | 108.59(18) |
| O(2)−Dy(1)−N(2) | 76.49(16) | O(7)−Dy(1)−O(6) | 79.16(16) |
| O(10)−Dy(1)−N(2) | 77.22(16) | O(3)−Dy(1)−O(2) | 78.21(16) |
| O(9)−Dy(1)−N(2) | 114.96(17) | O(6)−Dy(1)−O(2) | 137.70(16) |

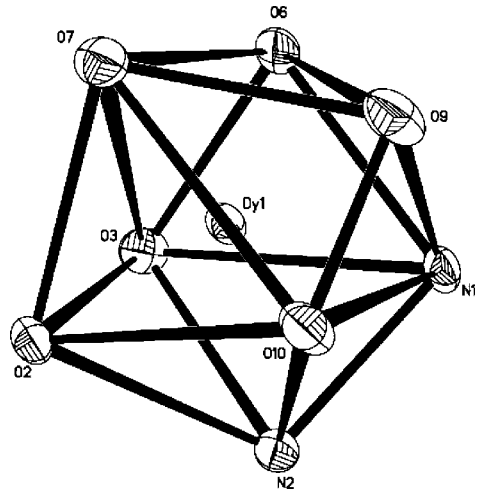


**Figure 3.** Coordination geometry of the $Dy^{3+}$ ion.

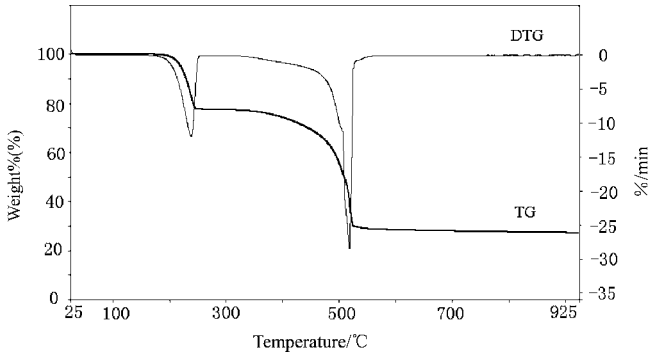


**Figure 4.** TG-DTG curves of the title complex at a heating rate of 15 $K \cdot min^{-1}$.

tion of $\nu_{CO}$ at 1688 $cm^{-1}$ in the free benzoic acid ligand completely disappears, while the asymmetric and symmetric absorption peaks at 1636 $cm^{-1}$ and 1407 $cm^{-1}$ appear in the spectra of the complex $[Dy(BA)_3bipy]_2$. These facts indicate that the oxygen atoms of benzoic acid are coordinated to the $Dy^{3+}$ ion.[25] Furthermore, the appearance of band $\nu$(Dy−O) at 427 $cm^{-1}$ also indicated that the oxygen atoms of the carboxylate group were coordinated to the Dy(III) ion. Meanwhile, the bands of $\nu_{CN}$ (1578 $cm^{-1}$), $\delta_{CC}$ (992 $cm^{-1}$), and $\delta_{CH}$ (757 $cm^{-1}$) of a bipy ligand shift to higher wavenumbers around at (1599, 1013, and 774) $cm^{-1}$ in the spectra of the complex, indicating that the nitrogen atoms of a bipy ligand are coordinated to the $Dy^{3+}$ ion.[9]

***Ultraviolet Spectra.*** The ligands and complex are soluble in DMSO solution. They have a strong $\pi \rightarrow \pi^*$ transition absorption. The UV absorption spectra of the complex show a maximum absorption peak at 280 nm, while the band for the benzoic acid ligand is at about 260 nm. This phenomenon can be explained by the expansion $\pi$-conjugated system that is caused by the metal coordination.[26] In addition, the maximum absorption band of bipy at 280 nm is similar to that in the complex. It is noteworthy that the molar extinction coefficient of bipy at 280 nm is 0.28, but in the complex it enhances to 0.35, suggesting that it has formed a bigger conjugated system than the ligand, namely forming a chelating ring.

***Crystal Structure Determination.*** As shown in Figure 2, the title complex shows an isolated binuclear structure. Crystal data collection and refinement data are listed in Table 3. The selected bond distances and angles are given in Table 4.

The two $Dy^{3+}$ ions are connected by four carboxylic groups through a bridging bidentate mode. Each $Dy^{3+}$ ion is linked by two oxygen atoms from one bidentate chelating carboxylic group, four oxygen atoms from four bridging bidentate carboxylic groups, and two nitrogen atoms from one bipy molecule. Figure 3 shows that the coordination polyhedron around $Dy^{3+}$ is a trigonal dodecahedron, and the coordination number of the dysprosium ion is eight.

In the title complex, the length of the Dy−O bond is in the range of 2.275(5) Å to 2.458(4) Å, and the mean bond length is 2.337 Å. The length of the Dy−N bond is between 2.560(3) Å and 2.605(3) Å with an average length of 2.583 Å, which is longer than that of the Dy−O bond. This fact shows that the Dy−O bond is stronger than the Dy−N bond.

Comparing with $[Sm(BA)_3bipy]_2$[27] and $[Eu(BA)_3bipy]_2$,[28] they are all binuclear molecules and have bidentate chelating and bridging bidentate carboxylic groups. However, the average distance of the Dy−O bond is 2.337 Å, and the mean bond distance of Dy−N is 2.583 Å in the title complex, slightly shorter than the corresponding average distance 2.364 Å (Eu−O) and 2.622 Å (Eu−N) of the $[Eu(BA)_3bipy]_2$ complex and 2.385 Å (Sm−O) and 2.637 Å (Sm−N) of the $[Sm(BA)_3bipy]_2$ complex, which is possibly related to the difference of the radius of $Eu^{3+}$, $Sm^{3+}$, and $Dy^{3+}$.

***Thermal Decomposition of the Title Complex.*** The TG-DTG curves of $[Dy(BA)_3bipy]_2$ at a heating rate of 15 $K \cdot min^{-1}$ are shown in Figure 4. The data of thermal decomposition are listed in Table 5. The SEM pictures of the complex $[Dy(BA)_3bipy]_2$ at 298 K, 570.61 K, and 1038.69 K are given in Figure 5(a−c).

As is shown in the DTG curve, the thermal decomposition process of the title complex can be divided into two stages. The first stage occurs from (434.97 to 570.61) K with a mass loss of 22.46 % (the theoretical mass loss is 22.90 %), which is equivalent to the loss of 2bipy. The degradation can be demonstrated by the bond distances of the structure of the title complex. From Table 4, it is easy to see that the Dy−N distance is longer than the Dy−O distance. Theoretically speaking, this bond is less stable and easily broken down. The IR spectra of the residue at 570.61 K show the disappearance of the absorption band of $\nu_{CN}$ at 1599 $cm^{-1}$. Compared with Figure 5(a) and Figure 5(b), the apparent form of the title complex changed from a smooth surface to a crackled crystal. The second stage occurs from (570.61 to 1038.69) K with a mass loss of 50.04 % (the theoretical mass loss is 49.75 %) corresponding to the loss of $C_{42}H_{30}O_9$. As shown in the IR spectra of the residue, the bands of the asymmetric vibrations $\nu_{as}(COO^-)$ at 1636 $cm^{-1}$ and symmetric vibrations $\nu_s(COO^-)$ at 1407 $cm^{-1}$ disappear. It can be seen that the crackled crystal broke up into even smaller granules as shown in Figure 5(c). The characteristic absorption band of the residue as shown in the IR spectra is similar to the standard sample spectrum of $Dy_2O_3$. Therefore, the final product

**Table 5. Thermal Decomposition Data for $[Dy(BA)_3bipy]_2$ ($\beta$ = 15 $K \cdot min^{-1}$)**

| | | | mass loss (%) | | | |
|---|---|---|---|---|---|---|
| stage | temperature range (K) | DTG peak temperature (K) | TG | theory | probable composition of removed groups | intermediate |
| I | 434.97 to 570.61 | 513.43 | 22.66 | 22.90 | 2bipy | $[Dy(BA)_3]_2$ |
| II | 570.61 to 1038.69 | 790.02 | 49.60 | 49.75 | $C_{42}H_{30}O_9$ | $Dy_2O_3$ |

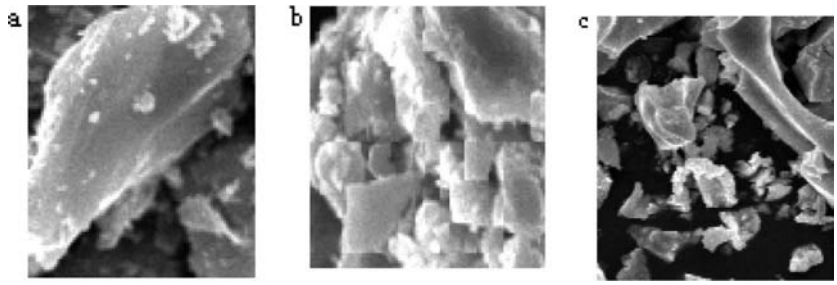


**Figure 5.** SEM pictures of the $[Dy(BA)_3bipy]_2$ at a, 298 K; b, 570.61 K; and c, 1038.69 K.

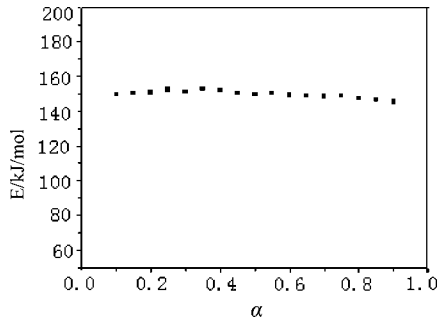


**Figure 6.** Relationship of $E$ and α of the first decomposition stage for the title complex.

at 1038.69 K is $Dy_2O_3$. The total weight loss of the thermal decomposition process of the title complex is 72.26 % (the theoretical mass loss is 72.65 %). On the basis of the above analysis, the thermal decomposition process of $[Dy(BA)_3bipy]_2$ can be denoted in the following scheme: $[Dy(BA)_3(bipy)]_2 \rightarrow [Dy(BA)_3]_2 \rightarrow Dy_2O_3$

***Kinetics of the First Decomposition Stage.*** The activation energy $E$ of the first decomposition stage has been calculated by the Starink method.[24] The equation is as follows

$$\ln \frac{\beta}{T_f^{1.92}} = -1.0008\frac{E}{RT_f} + C \quad (1)$$

where $\beta$ is the linear heating rate; $T_f$ is the absolute temperature; $R$ is the gas constant; $E$ is the activation energy; and $C$ is a constant. By substituting $T_f$ and $\beta$ obtained from the experiment into eq 1, $E$ is determined from the slope of plots of the $\ln(\beta/T_f^{1.92})$ versus $1/T_f$.

Figure 6 shows the relationship between $E$ and α. The activation energy $E$ changes slightly with the values of α, indicating the first decomposition stage is a single step reaction.[29] Therefore, the probable mechanism function and $E$, $A$ can be determined by means of a double equal-double steps method.[23] The Ozawa iteration equation[30] is as follows

$$\ln \frac{\beta}{H(x)} = \left\{\ln\left[\frac{0.0048AE}{R}\right] - \ln G(\alpha)\right\} - 1.0516\frac{E}{RT} \quad (2)$$

$$H(x) = \frac{\exp(-x)}{0.0048\exp(-1.0516x)}h(x)$$

$$h(x) = \frac{x^4 + 18x^3 + 86x^2 + 96x}{x^4 + 20x^3 + 120x^2 + 240x + 120}$$

$$\ln G(\alpha) = \ln\left(\frac{0.0048AEH(x)}{R}\right) - 1.0516\frac{E}{RT} - \ln\beta \quad (3)$$

where $G(\alpha)$ is the integral mechanism function; $T$ is the absolute temperature; $A$ is the pre-exponential factor; $R$ is the gas constant; $E$ is the apparent activation energy; and $\beta$ is the linear heating rate.

**Table 6. Conversion Degrees Measured for the Same Temperatures on the TG-DTG Curves of $[Dy(BA)_3bipy]_2$ at Different Heating Rates: Stage I**

| | α | | | | |
|---|---|---|---|---|---|
| $T$/K | $\beta = 3$ K·min$^{-1}$ | $\beta = 5$ K·min$^{-1}$ | $\beta = 7$ K·min$^{-1}$ | $\beta = 10$ K·min$^{-1}$ | $\beta = 15$ K·min$^{-1}$ |
| 475.91 | 0.2577 | 0.1714 | 0.1500 | 0.0911 | 0.0516 |
| 479.43 | 0.3369 | 0.2299 | 0.2000 | 0.1229 | 0.0697 |
| 482.19 | 0.4237 | 0.2860 | 0.2500 | 0.1531 | 0.0883 |
| 484.70 | 0.5073 | 0.3489 | 0.3000 | 0.1900 | 0.1097 |
| 486.79 | 0.5869 | 0.4090 | 0.3500 | 0.2259 | 0.1207 |
| 488.65 | 0.6694 | 0.4689 | 0.4000 | 0.2614 | 0.1520 |
| 490.21 | 0.7351 | 0.5263 | 0.4500 | 0.2943 | 0.1734 |

**Table 7. Partial Results from the Linear Least-Squares Method at Different Temperatures for $[Dy(BA)_3bipy]_2$: (Stage I)**

| $T$/K | function No. | $a$ | $b$ | $r$ |
|---|---|---|---|---|
| | 15 | 0.0118 | −0.7890 | −0.9819 |
| 475.91 | **28** | **−0.6105** | **−1.0333** | **−0.9812** |
| | 35 | 0.2653 | −0.7858 | −0.9667 |
| | 15 | 0.1208 | −0.7951 | −0.9820 |
| 479.43 | **28** | **−0.4744** | **−1.0344** | **−0.9810** |
| | 35 | 0.2949 | −0.7087 | −0.9590 |
| | 15 | 0.2231 | −0.8173 | −0.9846 |
| 482.19 | **28** | **−0.3490** | **−1.0550** | **−0.9834** |
| | 35 | 0.3046 | −0.6417 | −0.9534 |
| | 15 | 0.3075 | −0.8266 | −0.9871 |
| 484.70 | **28** | **−0.2490** | **−1.0577** | **−0.9855** |
| | 35 | 0.2903 | −0.5616 | −0.9442 |
| | 14 | 0.3617 | −0.7772 | −0.9846 |
| 486.79 | **28** | **−0.1306** | **−1.1096** | **−0.9823** |
| | 35 | 0.2913 | −0.5241 | −0.9214 |
| | 8 | −0.5964 | −1.6367 | −0.9761 |
| 488.65 | **28** | **0.0671** | **−1.0871** | **−0.9885** |
| | 35 | 0.2451 | −0.4274 | −0.9172 |
| | 6 | 0.1947 | −2.1449 | −0.9888 |
| 490.21 | **28** | **0.0060** | **−1.0992** | **−0.9897** |
| | 35 | 0.2189 | −0.3708 | −0.9052 |

By substituting the values of α and $\beta$ in Table 6 and various conversion functions[31] into eq 3, using the linear least-squares method with $\ln G(\alpha)$ versus $\ln \beta$, the linear correlation coefficient $r$, the slope $b$, and the intercept $a$ at the different temperatures were obtained. The partial results are listed in Table 7.

As seen from Table 7, it can be concluded that only the coefficients $r$ of the function No. 28 is best, while the slope $b$ is close to −1; so, the probable mechanism function of the title complex is $G(\alpha) = 1 - (1 - \alpha)^{1/4}$, $f(\alpha) = 4(1 - \alpha)^{3/4}$. The kinetic equation is $d\alpha/dt = A/\beta \exp(-E/RT)4(1-\alpha)^{3/4}$.

The value of the activation energy is inaccurate using plots of $\ln \beta$ versus $1/T$ based on the traditional isoconversional method, as it neglects the variation of $H(x)$ against $x$. However, iterative calculations considering the change can give the exact value of the activation energy by means of plots of $\ln(\beta/H)$ versus $1/T$, no matter how little or how great the $E/RT$ value of the reaction is. The value of activation energy is calculated by the Ozawa iteration method[30] according to eq 2, until the

**Table 8. Values of Temperatures at the Same Degree of Conversion for the Different Heating Rate on TG Curves for the Title Complex**

| | $T$ (K) | | | | |
|---|---|---|---|---|---|
| α | $\beta = 3$ K·min$^{-1}$ | $\beta = 5$ K·min$^{-1}$ | $\beta = 7$ K·min$^{-1}$ | $\beta = 10$ K·min$^{-1}$ | $\beta = 15$ K·min$^{-1}$ |
| 0.10 | 465.04 | 469.38 | 470.94 | 477.05 | 483.54 |
| 0.15 | 469.40 | 474.29 | 475.91 | 481.85 | 488.42 |
| 0.20 | 472.88 | 477.68 | 479.43 | 485.30 | 492.15 |
| 0.25 | 475.57 | 480.44 | 482.19 | 488.03 | 494.90 |
| 0.30 | 477.72 | 482.79 | 484.70 | 490.50 | 497.47 |
| 0.35 | 479.90 | 484.72 | 486.79 | 492.53 | 499.53 |
| 0.40 | 481.47 | 486.89 | 488.65 | 494.44 | 501.41 |
| 0.45 | 482.99 | 488.10 | 490.21 | 496.17 | 503.26 |
| 0.50 | 484.50 | 489.50 | 491.76 | 497.78 | 504.89 |
| 0.55 | 485.82 | 490.88 | 493.19 | 499.17 | 506.30 |
| 0.60 | 487.10 | 492.18 | 494.49 | 500.61 | 507.83 |
| 0.65 | 488.22 | 493.35 | 495.77 | 501.84 | 509.10 |
| 0.70 | 489.44 | 494.66 | 496.96 | 502.84 | 510.49 |
| 0.75 | 490.57 | 495.83 | 498.24 | 504.32 | 511.67 |
| 0.80 | 491.70 | 496.88 | 499.42 | 505.58 | 513.10 |
| 0.85 | 492.78 | 498.19 | 500.00 | 506.99 | 514.42 |
| 0.90 | 494.10 | 498.43 | 502.07 | 508.43 | 516.00 |

**Table 9. Values of the Kinetic Parameters Computed by Use of the Plot of ln $\beta/H(x)$ versus $1/T$**

| α | $E$ (kJ·mol$^{-1}$) | $A \cdot 10^{14}$/min$^{-1}$ | $r$ |
|---|---|---|---|
| 0.10 | 150.31 | 9.99 | −0.9778 |
| 0.15 | 151.29 | 13.13 | −0.9822 |
| 0.20 | 151.36 | 13.50 | −0.9815 |
| 0.25 | 152.95 | 20.51 | −0.9818 |
| 0.30 | 151.73 | 15.10 | −0.9839 |
| 0.35 | 153.52 | 23.77 | −0.9834 |
| 0.40 | 152.78 | 19.87 | −0.9854 |
| 0.45 | 150.93 | 12.60 | −0.9847 |
| 0.50 | 150.52 | 11.42 | −0.9848 |
| 0.55 | 150.93 | 12.75 | −0.9855 |
| 0.60 | 149.81 | 9.71 | −0.9847 |
| 0.65 | 149.55 | 9.23 | −0.9858 |
| 0.70 | 149.09 | 8.28 | −0.9849 |
| 0.75 | 149.66 | 9.63 | −0.9860 |
| 0.80 | 147.91 | 6.31 | −0.9854 |
| 0.85 | 147.00 | 5.10 | −0.9859 |
| 0.90 | 145.87 | 3.90 | −0.9862 |
| | 150.31 (average) | 12.05 (average) | |

absolute difference of $(E_i - E_{i-1})$ is less than a defined small quantity such as 0.1 kJ·mol$^{-1}$.

By substituting the values of α, $\beta$, and $T$ in Table 8 and the corresponding mechanism function determined above into eq 2, using the linear least-squares method with ln $\beta/H(x)$ versus $1/T$, the activation energy $E$ can be calculated from the value of the slope and the pre-exponential factor $A$ can also be calculated from the value of the intercept. The results are listed in Table 9.

The thermodynamic parameters of activation can be calculated from the equations[32,33]

$$A \exp(-E/RT) = \nu \exp(-\Delta G^{\neq}/RT) \quad (4)$$

$$\Delta H^{\neq} = E - RT \quad (5)$$

$$\Delta G^{\neq} = \Delta H^{\neq} - T\Delta S^{\neq} \quad (6)$$

where $\nu$ is the Einstein vibration frequency; $\Delta G^{\neq}$ is the Gibbs free enthalpy of activation; $\Delta H^{\neq}$ is the enthalpy of activation; and $\Delta S^{\neq}$ is the entropy of activation. The values of entropy, enthalpy, and the Gibbs free energy of activation at the peak temperature acquired on the basis of eqs 4 to 6 are shown in Table 10. As seen in Table 10, the values of $\Delta G^{\neq}$ are more than 0, indicating that the decomposition reaction for the title complex is not a spontaneous reaction.

**Table 10. Thermodynamic Parameters of the Title Complex**

| $\beta$ | $\Delta H^{\neq}$ | $\Delta G^{\neq}$ | $\Delta S^{\neq}$ | $T_P$ |
|---|---|---|---|---|
| K·min$^{-1}$ | kJ·mol$^{-1}$ | kJ·mol$^{-1}$ | J·mol$^{-1}$·K$^{-1}$ | K |
| 3 | 146.23 | 130.85 | 31.34 | 490.68 |
| 5 | 146.17 | 130.64 | 31.23 | 497.55 |
| 7 | 146.16 | 130.60 | 31.20 | 498.88 |
| 10 | 146.11 | 130.39 | 31.09 | 505.47 |
| 15 | 145.99 | 129.97 | 30.87 | 519.02 |

## Conclusions

The complex was synthesized by the reaction of $DyCl_3 \cdot 6H_2O$, benzoic acid and 2,2′-bipyridine. The crystal structure of $[Dy(BA)_3bipy]_2$ shows that the carboxylic groups are coordinated to $Dy^{3+}$ with bidentate chelating and bidentate bridging modes. The coordinate number is eight. The activation energy $E$, the pre-exponential factor $A$, the enthalpy of activation $\Delta H^{\neq}$, the Gibbs free energy of activation $\Delta G^{\neq}$, and the entropy of activation $\Delta S^{\neq}$ are 150.31 kJ·mol$^{-1}$, $12.05 \cdot 10^{14}$ min$^{-1}$, 145.99 kJ·mol$^{-1}$, 129.97 kJ·mol$^{-1}$, and 30.87 J·mol$^{-1}$·K$^{-1}$, respectively. The kinetic equation of the first step for the title complex is $d\alpha/dt = A/\beta \exp(-E/RT)4(1 - \alpha)^{3/4}$.

### Appendix A. Supporting Information

CCDC 686511 contains the supplementary crystallographic data for this paper. These data can be obtained free of charge via http://www.ccdc.cam.ac.uk/conts/retrieving.html, or from the Cambridge Crystallographic Data Centre, 12 Union Road, Cambridge CB2 1EZ, UK (fax: int.code +(1223)336-033; e-mail for inquiry: fileserv@ccdc.cam.ac.uk).

## Literature Cited


(1) Jin, L. P.; Lu, S. X.; Lu, S. Z. Crystal Structure and Spectra of Complex [Eu(o-ABA) $_3$bipy]bipy. *Polyhedron* **1996**, *15*, 4069–4077.

(2) Li, X.; Jin, L. P.; Wang, Y. H.; Lu, S. Z.; Zhang, J. H. {[Eu(*p*-MOBA) $_3 \cdot 2H_2O$]]$0.5H_2O \cdot 0.5$(4,4′-bipy))}$_\infty$. *Chin. J. Chem.* **2002**, *20*, 352–357.

(3) Li, Y.; Zheng, F. K.; Liu, X.; Zou, W. Q.; Guo, G. C.; Lu, C. Z.; Huang, J. S. Crystal Structures and Magnetic and Luminescent Properties of a Series of Homodinuclear Lanthanide Complexes with 4-Cyanobenzoic Ligand. *Inorg. Chem.* **2006**, *45*, 6308–6316.

(4) Li, X.; Zhang, Z. Y.; Song, H. B. Sythesis, Crystal Structure and Properties of Three New Holmiums 2-fluorobenzoato Complexes. *J. Mol. Struct.* **2005**, *751*, 33–40.

(5) Li, X.; Zhang, Z. Y.; Zou, Y. Q. Synthesis, Structure and Luminescence Properties of Four Novel Terbium2-Fluorobenzoate Complexes. *Eur. J. Inorg. Chem.* **2005**, *14*, 2909–2918.

(6) Wan, Y. H.; Zhang, L. P.; Jin, L. P.; Gao, S.; Lu, S. Z. High-Dimensional Archtectures from the Self-Assembly of Lanthanide Ions with Benzenedicarboxylates and 1,10-phenanthroline. *Inorg. Chem.* **2003**, *42*, 4985–4994.

(7) Li, G. Q.; Li, Y.; Zou, W. Q.; Chen, Q. Y.; Zheng, F. K.; Guo, G. C. Synthesis and Crystal Structure of a New Lanthanum(III) 4-Cyanobenzoate Complex. *Chin. J. Struct. Chem.* **2007**, *26*, 575–579.

(8) Niu, S. Y.; Jin, J.; Jin, X. L.; Yang, Z. Z. Synthesis, Strcture and Characterization of Gd(III) Dimer Bridged by Tetra Benzoates. *Solid State Sci.* **2002**, *4*, 1103–1106.

(9) Wang, R. F.; Jin, L. P.; Wang, M. Z.; Huang, S. H.; Chen, X. T. Synthesis, Crystal Structure and Luminescence of Coordination Compound of Europium p-Methylbenzoate with 2,2′-Dipyridine. *Acta Chim. Sinica* **1995**, *53*, 39–45.

(10) Wang, R. F.; Wang, S. P.; Shi, S. K.; Zhang, J. J. Crystal Structure and Properties of Terbium Benzoate Complex with 1,10-phenanthrolin. *Chin. J. Struct. Chem.* **2004**, *11*, 1300–1304.

(11) Wang, R. F.; Wang, S. P.; Shi, S. K.; Zhang, J. J. Crystal Structure and Properties of A Terbium m-methyl Benzoate Complex with 1,1-phenanthroline. *J. Coord. Chem.* **2002**, *55*, 215–223.

(12) Wang, R. F.; Wang, S. P.; Zhang, J. J. Crystal Structure and Properties of Complex [Eu(*m*-BrBA) $_3(H_2O) \cdot$(phen)]$_2$. *J. Mol. Struct.* **2003**, *648*, 151–158.

(13) Xu, X. L.; Zhang, J. J.; Yang, H. F.; Ren, N.; Zhang, H, Y. Synthesis, Crystal Structure and Thermal Decomposition of a Dysprosium(III) *p*-Fluorobenzoate 1,10-phenanthroline Complex. *J. Chem. Sci.* **2007**, *62b*, 51–54.

(14) Zhang, J. J.; Wang, R. F.; Wang, S. P.; Liu, H. M.; Li, J. B.; Bai, J. H. Kinetics and Lifetime of the Complex Terbium *p*- chlorobenzoate with 1,10-phenanthroline. *J. Therm. Anal. Calorim.* **2003**, *73*, 977–986.

(15) Xu, X. L.; Zhang, J. J.; Ren, N.; Zhang, H. Y. Preparation, Crystal Structure and Thermal Decomposition Mechanism of Complex [Dy(*p*-MOBA) $_3$phen]$_2$. *Russ. J. Coord. Chem.* **2007**, *33* (8), 622–626.

(16) Zhang, J. J.; Ren, N.; Bai, J. H.; Xu, S. L. Synthesis and Thermal Decomposition Reaction Kinetics of Complexes of [$Sm_2$(*m*-ClBA) $_6$(phen) $_2$] · $2H_2O$ and [$Sm_2$(*m*-BrBA) $_6$(phen) $_2$]·$2H_2O$. *J. Chem. Kinet.* **2007**, *39*, 67–74.

(17) Ren, N.; Zhang, J. J.; Guo, Y. H.; Sun, M. Q.; Xu, S. L.; Zhang, H. Y. Non-isothermal Decomposition Kinetics of Complexes [Sm(*m*-MBA) $_3$ phen]$_2$ and [Sm(*o*-MOBA) $_3$ phen]$_2$·$2H_2O$. *Chem. Res. Chin. U* **2007**, *23*, 489–492.

(18) Zhang, J. J.; Ren, N.; Xu, S. L. Synthesis and Thermal Decomposition Kinetics of the Complex of Samrium p-Methybenzoate with 1,10-Phenanthroline. *Chin. J. Chem.* **2007**, *25*, 125–128.

(19) Zhang, J. J.; Wang, R. F.; Wang, S. P.; Liu, H. M.; Li, J. B.; Bai, J. H.; Ren, N. Preparation, Thermal Decomposition Process and Kinetics for Terbium*p*-methoxybenzoate Ternary Complex with 1,10-phenathroline. *J. Therm. Anal. Calorim.* **2005**, *79*, 181–186.

(20) Zhang, J. J.; Wang, R. F.; Liu, H. M.; Li, J. B.; Ren, N.; Gao, Z. H. Non-isothermal Kinetics of the First-stage Decomposition Reaction of the Complex of Terbium p-Methylbenzoate with 1,10--phenathroline. *Chin. J. Chem.* **2005**, *23*, 646–650.

(21) Ren, N.; Zhang, J. J.; Xu, S. L.; Wang, R. F.; Wang, S. P. Crystal Structure and Thermal Decomposition of Complex [Sm(*o*-MBA) $_3$phen]$_2$. *Thermochim. Acta* **2005**, *438*, 172–177.

(22) Ren, N.; Zhang, J. J.; Wang, R. F.; Wang, S. P. Synthesis, Crystal Structure and Thermal Decomposition Process of Complex [Sm(BA) $_3$phen]$_2$. *J. Chin. Chem. Soc.* **2006**, *53* (2), 293–298.

(23) Zhang, J. J.; Ren, N. A New Kinetic Method of Processing TA Data. *Chin. J. Chem.* **2004**, *22*, 1459–1462.

(24) Starink, M. J. The Determination of Activation Energy from Linear Heating Rate Experiments: A Comparison of the Accuracy of Isoconversion Methods. *Thermochim. Acta* **2003**, *404*, 163–176.

(25) Shi, Y. Z.; Sun, X. Z.; Jiang, Y. H. *Spectra and Chemical Identification of Organic Compounds*; Science and technology Press: Nanjing, 1988; p 98.

(26) An, B. L.; Gong, M. L.; Li, M. X.; Zhang, J. M. Synthesis, Structure and Luminescence Properties of Samarium(III) and Dysprosium(III) Complexes with a New Tridentate Organic Ligand. *J. Mol. Struct.* **2004**, *687*, 1–6.

(27) Zhang, H. Y.; Wu, K. Z.; Zhang, J. J.; Xu, S. L.; Ren, N.; Bai, J. H.; Tian, L. Synthesis, Crystal Structure and Thermal Decomposition Kinetics of the Complex [Sm(BA) $_3$bipy]$_2$. *Synth. Metal* **2008**, *158*, 157–164.

(28) Zhang, Y.; Jin, L. P.; Lǔ, S. Z. Crystal Structure and Luminescence of [Eu $_2$(BA) $_6$(bipy) $_2$]. *J. Inorg. Chem. (in Chinese)* **1997**, *13*, 280–287.

(29) Lu, Z. R.; Ding, Y. C; Xu, Y.; Li, B. L.; Zhang, Y. TA Study on Four One-Dimensional Chain Copper Complexes with Benzoylacetone or 1,1,1-Trifluoro-3-(2-thenoyl)-acetone Bridged through Azobispyridine Ligands. *J. Inorg. Chem. (in Chinese)* **2005**, *21*, 181–185.

(30) Gao, Z.; Nakada, M.; Amasski, I. A Consideration of Errors and Accuracy in the Isoconversional Methods. *Thermochim. Acta* **2001**, *369*, 137–142.

(31) Hu, R. Z.; Gao, S. L.; Zhao, F. Q.; Shi, Q. Z.; Zhang, T. L.; Zhang, J. J. *Thermal Analysis Kinetics*, 2nd ed.; Science Press: Beijing, 2008; p 151.

(32) Straszko, J.; Olstak-Humienik, M.; Mozejko, J. Kinetics of Thermal Decomposition of $ZnSO_4$·$7H_2O$. *Thermochim. Acta* **1997**, *292*, 145–150.

(33) Olstak-Humienik, M.; Mozejko, J. Thermodynamic Functions of Activated Complexes Created in Thermal Decomposition Processes of Sulphates. *Thermochim. Acta* **2000**, *344*, 73–79.

Received for review August 3, 2008. Accepted October 25, 2008. This project was supported by the National Natural Science Foundation of China (No.20773034), the Natural Science Foundation of Hebei Province (No.B2007000237) and Science Foundation of Hebei Normal University (No. L2006Z06).

JE8006106